



LJMU Research Online

Wilding, CS and Weedall, GD

Morphotypes of the common beadlet anemone *Actinia equina* (L.) are genetically distinct

<http://researchonline.ljmu.ac.uk/id/eprint/9618/>

Article

Citation (please note it is advisable to refer to the publisher's version if you intend to cite from this work)

Wilding, CS and Weedall, GD (2018) Morphotypes of the common beadlet anemone *Actinia equina* (L.) are genetically distinct. *Journal of Experimental Marine Biology and Ecology*, 510. pp. 81-85. ISSN 0022-0981

LJMU has developed **LJMU Research Online** for users to access the research output of the University more effectively. Copyright © and Moral Rights for the papers on this site are retained by the individual authors and/or other copyright owners. Users may download and/or print one copy of any article(s) in LJMU Research Online to facilitate their private study or for non-commercial research. You may not engage in further distribution of the material or use it for any profit-making activities or any commercial gain.

The version presented here may differ from the published version or from the version of the record. Please see the repository URL above for details on accessing the published version and note that access may require a subscription.

For more information please contact researchonline@ljmu.ac.uk

<http://researchonline.ljmu.ac.uk/>

1 Accepted for publication in Journal of Experimental Marine Biology and Ecology

2

3 **Morphotypes of the common beadlet anemone *Actinia equina* (L.) are genetically distinct**

4

5 **Running head: mtDNA of *Actinia equina***

6

7 Craig S. Wilding¹ and Gareth D. Weedall.

8

9 School of Natural Sciences and Psychology,

10 Liverpool John Moores University,

11 Liverpool,

12 L3 3AF.

13 UK.

14 1: Corresponding author

15

16

17 Keywords: Cnidaria, sea anemone, beadlet anemone, *Actinia equina*, barcoding, *COI*

18 **Abstract**

19 Anemones of the genus *Actinia* are ecologically important and familiar organisms on many rocky
20 shores. However, this genus is taxonomically problematical and prior evidence suggests that the
21 North Atlantic beadlet anemone, *Actinia equina*, may actually consist of a number of cryptic species.
22 Previous genetic work has been largely limited to allozyme electrophoresis and there remains a
23 dearth of genetic resources with which to study this genus. Mitochondrial DNA sequencing may help
24 to clarify the taxonomy of *Actinia*. Here, the complete mitochondrial genome of the beadlet
25 anemone *Actinia equina* (Cnidaria: Anthozoa: Actinaria: Actiniidae) is shown to be 20,690bp in
26 length and to contain the standard complement of Cnidarian features including 13 protein coding
27 genes, two rRNA genes, two tRNAs and two Group I introns, one with an in-frame truncated homing
28 endonuclease gene open reading frame. However, amplification and sequencing of the standard
29 mtDNA barcoding region of the *cytochrome oxidase 1* gene revealed only two haplotypes, differing
30 by a single base pair, in widely geographically separated *A. equina* and its congener *A. prasina*. *COI*
31 barcoding shows that whilst *A. equina* and *A. prasina* share the common mtDNA haplotype,
32 haplotype frequency differed significantly between *A. equina* with red/orange pedal discs and those
33 with green pedal discs, consistent with the hypothesis that these morphotypes represent incipient
34 species.

35 **Introduction:**

36 The Cnidarian genus *Actinia* (Cnidaria: Anthozoa: Actinaria: Actiniidae) is notably diverse,
37 phenotypically variable and has had a fluid taxonomical history (Perrin et al., 1999). The beadlet
38 anemone, *Actinia equina* is a common organism of North Atlantic rocky shores but has a reported
39 range from the Kola Peninsula of northern Russia to the coast of South Africa (Manuel, 1988;
40 Stephenson, 1935). Additionally, populations of *Actinia* in the Adriatic, Mediterranean and Black Sea
41 (Schama et al., 2005; Schmidt, 1971) have been ascribed to *A. equina*, as have animals from the
42 coasts of Japan (Honma et al., 2005; Yanagi et al., 1999), Korea (Song, 1984) and Hong Kong (Morton
43 and Morton, 1983). Allozyme electrophoresis studies have suggested that *Actinia* from some
44 geographically distinct populations represent separate species, now labelled *A. schmidti*
45 (Mediterranean), *A. cari* (Mediterranean), *A. sali* (Cape Verde), *A. nigropuncta* (Madeira) and an, as
46 yet, unnamed form from South Africa (Monteiro et al., 1997; Perrin et al., 1999; Schama et al.,
47 2005). Whether other populations of animals currently labelled as *A. equina* are misidentified cryptic
48 species, or truly represent extensions to the known geographic range of this species, has not yet
49 been assessed. Even within British populations of *Actinia equina*, the tremendous diversity in colour
50 of *Actinia* individuals has led to taxonomic confusion. Allozyme electrophoresis studies have
51 demonstrated the specific status of the strawberry anemone *A. fragacea* (Carter and Thorpe, 1981)
52 and suggested that the green-columned form is a separate species from *A. equina*, now labelled *A.*
53 *prasina* (Sole-Cava and Thorpe, 1987) although see Schama et al. (2005), but additional cryptic
54 species perhaps also exist, particularly those morphotypes that differ in the colour of the pedal disc
55 (grey/green versus red/pink/orange). These morphotypes show clear differences in intertidal
56 distribution (red/pink morphs are found higher up the shore with green/grey morphs lower down
57 the intertidal zone) and have been shown to present diagnostic allozyme genotypes at both malate
58 dehydrogenase and hexokinase loci (Quicke and Brace, 1984; Quicke et al., 1983). In addition, they
59 exhibit significant differences in aggression, nematocyst morphology, adhesion, and settlement
60 patterns (Brace and Reynolds, 1989; Collins et al., 2017; Perrin et al., 1999; Quicke and Brace, 1984;

61 Quicke et al., 1983; Quicke et al., 1985; Watts and Thorpe, 1998). *Actinia* remains a key and common
62 ecological species within the intertidal zone (Collins et al., 2017; Perrin et al., 1999; Schama et al.,
63 2005) and hence accurate understanding of its taxonomy and the ability to identify species is
64 important for understanding the functional ecology of this environment.

65 Due to the taxonomic confusion surrounding this genus and the difficulties in applying
66 morphological taxonomy to such soft-bodied animals, the study of mitochondrial DNA may aid in
67 resolution of this problematical taxon. Whilst there is an increasing number of complete
68 mitochondrial genomes from the phylum e.g. (Beagley et al., 1998; Chi et al., 2018; Foox et al., 2016;
69 Zhang and Zhu, 2017), none is currently available from the genus *Actinia*. Application of
70 mitochondrial DNA barcoding (Ratnasingham and Hebert, 2007) also seems a promising tool.
71 However, the evolutionary rate of mtDNA in Cnidaria is considered to be low (Huang et al., 2008;
72 Shearer et al., 2002) potentially presenting difficulties for the application of this methodology. DNA
73 barcoding relies on the use of standard primers which for metazoans are typically those of Folmer et
74 al. (1994) which target the *cytochrome oxidase subunit I* gene. However, the utility of *COI*, and
75 whether other regions of the mtDNA molecule harbour more variation, remains untested.

76 As part of a study to generate a full reference genome for *A. equina* to facilitate investigation of the
77 genomic basis of differentiation among beadlet anemone morphotypes, the complete mitochondrial
78 genome of *Actinia equina* is reported here and the utility of mitochondrial DNA barcoding for
79 studying intraspecific variation of British populations assessed.

80

81 **Materials and Methods:**

82 A single specimen of *Actinia equina* (with a red column and red pedal disc) was collected from
83 Rhosneigr, Anglesey, North Wales, UK and kept in artificial seawater at 8°C for two weeks to allow it
84 to purge of any food which may have contaminated extracted DNA. Prior to DNA extraction, the
85 animal was inspected to ensure that there were no intra-gastrovascular cavity brooded offspring
86 which may have introduced additional haplotypes into the extracted DNA (although evidence to

87 date suggests these would be clonal (Pereira et al., 2017)). It was then minced with a scalpel and
88 ground under liquid nitrogen. The resultant powder was added to 20ml 80 mM EDTA (pH 8.0), 100
89 mM Tris-HCl (pH 8.0), 0.5% SDS, 100 µg/mL proteinase K, and 40µl RNaseA (100mg/ml) and
90 incubated at 60°C for 3 hours. Genomic DNA was isolated from this solution by salt-chloroform
91 extraction (Müllenbach et al., 1989), precipitated with 0.6 volumes of isopropanol, and dissolved in
92 water. Extracted DNA was further purified using a Qiagen Genomic Tip 20/G following the
93 manufacturer's instructions and precipitated a second time with 0.6 volumes of isopropanol.
94 20kb-insert PacBio sequencing libraries were produced and sequenced on 5 SMRT cells on a Pacific
95 Biosciences Sequel (Pacific Biosciences, Menlo Park, CA, USA) at the Centre for Genomic Research,
96 University of Liverpool.

97 Sequencing produced 3,507,426 'polymerase reads' (single reads that can cover the same insert
98 multiple times) that were split into a total of 4,936,001 subreads (full or partial passes of the same
99 insert). Of these subreads, 487,629 were longer than 20 kb and 1,409,598 longer than 10 kb.

100 All subreads were assembled using CANU v1.7 (Koren et al., 2017) with default parameters for
101 PacBio data. To identify mitochondrial DNA, all assembled contigs were used to make a BLAST
102 database using BLAST+ v2.2.28 (Camacho et al., 2009). This was queried using BLASTn with two
103 published *A. equina* mitochondrial genes: a partial cytochrome B-like gene (*cytB*; GenBank accession
104 [DQ683369.1](#)) and a sequence containing the *cytochrome oxidase subunit I* gene (*COI*) and *homing*
105 *endonuclease* gene (*HEG*) (GenBank accession [DQ831335.1](#)). To check for errors in the final
106 mitochondrial genome sequence, all subreads were aligned to the sequence using bwa v0.7.12-
107 r1039 (Li and Durbin, 2009), using the bwa-mem algorithm with default parameters.

108 Initial annotation of mitochondrial genome features used MITOS (Bernt et al., 2013) with manual
109 annotation conducted to finalise gene models. tRNA genes identified by MITOS were further
110 investigated using tRNAscan (Lowe and Chan, 2016). Gene order was depicted using MTVIZ
111 (<http://pacosy.informatik.uni-leipzig.de/mtviz>) and G/C content depicted with CGView (Stothard and
112 Wishart, 2005). Sequence divergence between the mitochondrial genomes of *A. equina* and *A. viridis*

113 (accession number [KY860669](#)) was estimated for a 500 bp sliding window, moving in steps of 25 bp
114 across the mitochondrial genome, using DNASp v6 (Rozas et al., 2017).

115 **DNA barcoding**

116 *A. equina* ($N = 43$) and *A. prasina* ($N = 3$) were collected from a range of locations around the UK and
117 the Isle of Man (Table 1) leaving at least 2m between samples from the same shore to avoid
118 sampling clones. DNA was extracted from tentacle samples using a GeneJet Genomic DNA extraction
119 kit (ThermoFisher, UK). Partial *COI* fragments were amplified using the primers of Folmer et al.
120 (1994) at 0.2 μ M using 1x GoTaq HS mastermix (Promega) with cycling conditions of 95°C for 3 min
121 followed by 35 cycles of 95°C for 1 min, 40°C for 1 min, and 72°C for 1.5 mins, followed by a final
122 extension step at 72°C for seven minutes. Alternative primers were used to amplify a 559bp section
123 of the intergenic region between *COIII* and *COI* (5'-cggggttttcatggtctgcat-3' and 5'-
124 ccaggggcagataactccaa-3') and a 598bp region between *COI* and *ND4* (5'-
125 cccgcctttgtctcact-3' and 5'-caccataattgccagcccaa-3'), designed using
126 Primer3 (Untergasser et al., 2012). PCRs were undertaken using 1x GoTaq HS mastermix with cycling
127 conditions of 5 min at 94°C followed by 35 cycles of 94°C for 30 sec, 55°C for 30 sec and 72°C for 1
128 min and a final extension time of 72°C for 5 min with PCR products purified using a GeneJet PCR
129 purification kit and sequenced by GATC Biotech, Konstanz, Germany. Sequences were aligned using
130 ClustalW (Larkin et al., 2007).

131

132 **Results**

133 Both BLASTn searches (with default parameters) returned a single contig (41,948 bp) but each query
134 sequence aligned to the contig more than once (which can occur when a circular sequence is
135 assembled). The first position of the *cytB* sequence (positions 6,928 and 27,619 in tig00010800) was
136 used to trim the contig into a full-length putative mitochondrial genome of 20,690 bp which was
137 then reoriented with the first base of *ND5* at base 1. 8,996 subreads could be aligned back to this
138 sequence with a median coverage depth of 2,044.

139 This genome contains the standard 13 protein coding genes typical of the mitochondrial DNA, two
140 ribosomal subunits (small and large) and, in line with other Cnidarian genomes, just two transfer
141 RNAs (tryptophan and methionine) (Figure 1). In addition, an open reading frame (*OrfA*) potentially
142 encoding a 645 amino acid protein was located between *COII* and *ND4*. As for other Cnidaria, type I
143 introns were found within *ND5* (with *ND1* and *ND3* within the intron) and *COI* (containing a
144 truncated *homing endonuclease* gene (*HEG*) ORF). The *HEG* of *A. equina* has an ORF of 343 amino
145 acids, slightly longer than that of *A. viridis* (339 amino acids). This is due to a single base insertion
146 relative to the ORF of *A. viridis*, with a 6 base poly-A tract at positions 17,646-17,651 at which *A.*
147 *viridis* has a 5bp poly-A tract. The insertion was confirmed by Sanger sequencing of PCR products.
148 The region between *ND3* and *ND5* displayed a partial ORF with similarities to *ND5* and it appears
149 likely that this is pseudogenic. The mitochondrial genome was 61.02% A/T although this varied
150 across the genome (Figure 1). The complete sequence has been deposited in Genbank with
151 accession number **MH545699**.

152 Sequencing of PCR amplicons of the standard barcoding region of *COI* using the primers of Folmer et
153 al. (1994) showed that beadlet anemone samples collected from England, Scotland, Wales and the
154 Isle of Man displayed only two haplotypes (Table 1, Figure 2) which differed by just 1bp, a G-A
155 synonymous transition at position 16,941 (Haplotype A accession number: **MH636618**; Haplotype B
156 accession number: **MH636619**). Whilst variation was low, haplotype A was only ever seen in *A.*
157 *equina* with red or orange pedal discs and never in animals with green pedal discs or in *A. prasina*
158 and this association between haplotype and *A. equina* colour morph was significant ($\chi^2 = 16.43$; $P <$
159 0.0001).

160 Sliding window analysis comparing the complete *A. equina* mitochondrial genome to the complete
161 mitochondrial genome of *Anemonia viridis* revealed low sequence divergence, with the exception of
162 the intergenic regions separating *COIII* and *COI*, and between *COI* and *ND4* (Figure 3). Using primers
163 designed to amplify these regions of maximum interspecific divergence then, as for *COI*, intraspecific
164 variation among *A. equina* in these regions was low with a single haplotype in the intergenic

165 fragment between *COI* and *ND4* (accession number MH686230) and just two haplotypes (accession
166 numbers MH686231-MH686232), differing by two base pairs, for the fragment between *COIII* and
167 *COI* (an A-T transversion at position 16,432 resulting in an I-L amino acid change in *COIII* and an
168 intergenic C-T transition at 16,517).

169

170 **Discussion**

171 The mitochondrial genome of *Actinia equina* has the standard mitochondrial gene order typical of
172 Cnidaria (Beagley et al., 1998; Chi et al., 2018; Fook et al., 2016) although at 20,690bp the mtDNA is
173 slightly longer than that of other Cnidaria, largely due to an increased intergenic region between
174 *ND3* and the second exon of *ND5*. This region contains a partial pseudogene of *ND5* as seen also in
175 *Bolocera tuediae* (Emblem et al., 2014). As in *A. viridis* (Chi et al., 2018), the homing endonuclease
176 gene of *A. equina* is fused in-frame with *COI* (Chi et al. 2018) but differs at the 3' end due to an
177 insertion in a poly-A tract resulting in a frameshift.

178 Whole mitochondrial DNA sequences have been used to study Cnidarian phylogeny e.g. (Emblem et
179 al., 2014; Fook et al., 2016) but individual mitochondrial genes are often used in studies of
180 phylogenetics and population studies with the *cytochrome oxidase subunit I* the most common
181 target. Here, sequencing of *COI* from *A. equina* samples collected from Scotland, Wales, England and
182 the Isle of Man, and including individuals of *A. prasina* deemed a separate species based on allozyme
183 evidence (Sole-Cava and Thorpe, 1987), detected only two haplotypes differing by just one base pair.
184 *A. prasina* shared the same haplotype as *A. equina* with a green pedal disc. It seems therefore that
185 the low variability of *COI* makes this gene of little use for population genetic studies. However, the
186 fact that haplotype A was seen only in animals with red/orange pedal discs, and never in those with
187 green pedal discs adds weight to the argument that these may represent incipient species (Collins et
188 al., 2017; Perrin et al., 1999; Quicke et al., 1983). This low variability of mitochondrial DNA has been
189 seen previously: Pereira et al. (2014), studying the mitochondrial *16S* gene, found only two
190 haplotypes among 77 anemones from the coast of Portugal. It is extremely surprising that in a

191 species considered largely to reproduce through budding, and in which little evidence of sexual
192 reproduction has been found (Perrin et al., 1999), there is such a dearth of variability in the
193 mitochondrial genome across large geographic scales. In addition, the lack of difference in sequence,
194 or haplotype frequency, between *A. equina* and *A. prasina* is surprising. However, allozyme studies
195 of genetic distance find levels appropriate for interspecific comparisons when *A. prasina* is compared
196 to *A. equina* with a red pedal disc, but not when compared to samples with a grey pedal disc
197 (Schama et al., 2005) further suggesting that what is currently regarded as *A. equina* encompasses at
198 least two cryptic species. Other mitochondrial genes may be more variable and hence of more utility
199 for population genetics/phylogenetics. Emblem et al. (2014) demonstrated in interspecific
200 comparisons that of the protein coding complement of the mtDNA the *HEG* has the highest
201 evolutionary rate. However, previous work showed no intraspecific variation in the *HEG* sequence
202 when 95 individuals of the Anthozoan *Metridium senile* were compared (Goddard et al., 2006).
203 Intergenic regions of the mtDNA which are likely less constrained by selection pressures may be of
204 use and we show through comparison of sequence divergence between *A. equina* and *A. viridis*
205 across the whole molecule that two intergenic regions of the mitochondrial genome have maximum
206 divergence and hence hold promise as phylogenetic and population genetic markers. However, we
207 show through sequencing of *A. equina* and *A. prasina* individuals that within these species there are
208 few variable positions within these two regions, so they are of no more utility than the *COI*
209 barcoding region. Taken together, this suggests that the low inherent mutation rate of this molecule
210 make it uninformative for understanding the complex relationships within this genus or the
211 population genetics of the inherent species, and that nuclear DNA studies will instead need to be
212 conducted. Nevertheless, the significant difference in haplotype frequencies between red/orange
213 and green pedal disc anemones does add to the growing evidence from aggression, nematocyst
214 morphology, distribution and allozyme data (Collins et al., 2017; Perrin et al., 1999; Quicke et al.,
215 1983) that these may be incipient species. The causes of speciation in intertidal organisms have been
216 most intensively studied in the rough periwinkle *Littorina saxatilis* where 'crab' and 'wave'

217 morphotypes appear to be selected by the action of predator pressure (from crabs) and wave action
218 (Butlin et al., 2014) and the genomic regions under selection are now being revealed (Westram et
219 al., 2018). Wave action appears also to be a factor in speciation in other organisms, e.g. kelp (Augyte
220 et al., 2018). However, the intertidal zone is characterized by a range of strong divergent selective
221 pressures, both biotic and abiotic and such extreme stresses (as those imposed on intertidal
222 organisms) can be sufficient to promote speciation (Lexer and Fay, 2005). The fact that anemones
223 with red/orange pedal discs are found higher up the intertidal zone than those with green pedal
224 discs (Perrin et al., 1999; Quicke and Brace, 1984; Quicke et al., 1983), and that differences are
225 present in adhesion strength and preference for substratum orientation, with red pedal disc forms
226 preferring more vertical surfaces than the green pedal disc form (Quicke and Brace, 1984; Quicke et
227 al., 1983), indicates that ecological factors may indeed be driving speciation. In other Cnidarians
228 ecological specialization is a driver of speciation (González et al., 2018) and this may also be the case
229 for *Actinia*. The precise nature of the selective pressures on anemone populations remain to be
230 elucidated but the availability of genetic and genomic resources (Wilding and Weedall, unpublished)
231 for this widely-studied species will greatly aid in our efforts to understand the extent and pattern of
232 differentiation in this ecologically important animal.

233

234 **Acknowledgments**

235 This work was supported by an award from the Liverpool John Moores University – Technology
236 Directorate Voucher Scheme providing access to University of Liverpool’s Shared Research Facilities.

237 We thank Jeremy Hussey and John Halsall for assistance in the collections from the Isle of Man and
238 Stefano Mariani for help with the Pembrokeshire collections.

239

240 **References**

241 Augyte, S., Lewis, L., Lin, S., Neefus, C.D., Yarish, C., 2018. Speciation in the exposed intertidal zone:
242 the case of *Saccharina angustissima* comb. nov. & stat. nov. (Laminariales, Phaeophyceae).
243 Phycologia 57, 100-112.

244 Beagley, C.T., Okimoto, R., Wolstenholme, D.R., 1998. The mitochondrial genome of the sea
245 anemone *Metridium senile* (Cnidaria): introns, a paucity of tRNA genes, and a near-standard genetic
246 code. Genetics 148, 1091-1108.

247 Bernt, M., Donath, A., Jühling, F., Externbrink, F., Florentz, C., Fritzschn, G., Pütz, J., Middendorf, M.,
248 Stadler, P.F., 2013. MITOS: Improved de novo metazoan mitochondrial genome annotation. Mol.
249 Phylogenet. Evol. 69, 313-319.

250 Brace, R.C., Reynolds, H.A., 1989. Relative intraspecific aggressiveness of pedal disc colour
251 phenotypes of the beadlet anemone, *Actinia equina*. J. Mar. Biol. Assoc. U.K. 69, 273-278.

252 Butlin, R.K., Saura, M., Charrier, G., Jackson, B., André, C., Caballero, A., Coyne, J.A., Galindo, J.,
253 Grahame, J.W., Hollander, J., Kempainen, P., Martínez-Fernández, M., Panova, M., Quesada, H.,
254 Johannesson, K., Rolán-Alvarez, E., 2014. Parallel evolution of local adaptation and reproductive
255 isolation in the face of gene flow. Evolution 68, 935-949.

256 Camacho, C., Coulouris, G., Avagyan, V., Ma, N., Papadopoulos, J., Bealer, K., Madden, T.L., 2009.
257 BLAST+: architecture and applications. BMC Bioinformatics 10, 421.

258 Carter, M.A., Thorpe, J.P., 1981. Reproductive, genetic and ecological evidence that *Actinia equina*
259 var. *mesembryanthemum* and var. *fragacea* are not conspecific. J. Mar. Biol. Assoc. U.K. 61, 79-93.

260 Chi, S.I., Urbarova, I., Johansen, S.D., 2018. Expression of homing endonuclease gene and insertion-
261 like element in sea anemone mitochondrial genomes: Lesson learned from *Anemonia viridis*. Gene
262 652, 78-86.

263 Collins, J.R., Vernon, E.L., Thomson, J.S., 2017. Variation in risk-taking and aggression in morphotypes
264 of the beadlet anemone, *Actinia equina* (L.), and the green anemone, *Actinia prasina* (Gosse). J. Exp.
265 Mar. Biol. Ecol. 496, 29-36.

266 Emblem, Å., Okkenhaug, S., Weiss, E.S., Denver, D.R., Karlsen, B.O., Moum, T., Johansen, S.D., 2014.
267 Sea anemones possess dynamic mitogenome structures. *Mol. Phylogenet. Evol.* 75, 184-193.

268 Folmer, O., Black, M., Hoeh, W., Lutz, R., Vrijenhoek, R., 1994. DNA primers for the amplification of
269 mitochondrial *cytochrome oxidase subunit I* from diverse metazoan invertebrates. *Mol. Mar. Biol.*
270 *Biotechnol.* 3, 294-299.

271 Foox, J., Brugler, M., Siddall, M.E., Rodríguez, E., 2016. Multiplexed pyrosequencing of nine sea
272 anemone (Cnidaria: Anthozoa: Hexacorallia: Actiniaria) mitochondrial genomes. *Mitochondrial DNA*
273 *Part A* 27, 2826-2832.

274 Goddard, M.R., Leigh, J., Roger, A.J., Pemberton, A.J., 2006. Invasion and persistence of a selfish
275 gene in the Cnidaria. *PLoS ONE* 1, e3.

276 González, A.M., Prada, C.A., Ávila, V., Medina, M., 2018. Ecological speciation in corals, in: Oleksiak,
277 M.F., Rajora, O.P. (Eds.), *Population Genomics: Marine Organisms*. Springer.

278 Honma, T., Minagawa, S., Nagai, H., Ishida, M., Nagashima, Y., Shiomi, K., 2005. Novel peptide toxins
279 from acrorhagi, aggressive organs of the sea anemone *Actinia equina*. *Toxicon* 46, 768-774.

280 Huang, D., Meier, R., Todd, P.A., Chou, L.M., 2008. Slow mitochondrial *Col* sequence evolution at the
281 base of the metazoan tree and its implications for DNA barcoding. *J. Mol. Evol.* 66, 167-174.

282 Koren, S., Walenz, B.P., Berlin, K., Miller, J.R., Bergman, N.H., Phillippy, A.M., 2017. Canu: scalable
283 and accurate long-read assembly via adaptive *k*-mer weighting and repeat separation. *Genome Res.*
284 27, 722-736.

285 Larkin, M.A., Blackshields, G., Brown, N.P., Chenna, R., McGettigan, P.A., McWilliam, H., Valentin, F.,
286 Wallace, I.M., Wilm, A., Lopez, R., Thompson, J.D., Gibson, T.J., Higgins, D.G., 2007. Clustal W and
287 Clustal X version 2.0. *Bioinformatics* 23, 2947-2948.

288 Lexer, C., Fay, M.F., 2005. Adaptation to environmental stress: a rare or frequent driver of
289 speciation? *J. Evol. Biol.* 18, 893-900.

290 Li, H., Durbin, R., 2009. Fast and accurate short read alignment with Burrows–Wheeler transform.
291 *Bioinformatics* 25, 1754-1760.

292 Lohse, M., Drechsel, O., Kahlau, S., Bock, R., 2013. OrganellarGenomeDRAW—a suite of tools for
293 generating physical maps of plastid and mitochondrial genomes and visualizing expression data sets.
294 Nucleic Acids Res. 41, W575-W581.

295 Lowe, T.M., Chan, P.P., 2016. tRNAscan-SE On-line: integrating search and context for analysis of
296 transfer RNA genes. Nucleic Acids Res. 44, W54-W57.

297 Manuel, R.L., 1988. British Anthozoa. E.J. Brill, Leiden.

298 Monteiro, F.A., Solé-Cava, A.M., Thorpe, J.P., 1997. Extensive genetic divergence between
299 populations of the common intertidal sea anemone *Actinia equina* from Britain, the Mediterranean
300 and the Cape Verde Islands. Marine Biology 129, 425-433.

301 Morton, B., Morton, J., 1983. The sea shore ecology of Hong Kong. Hong Kong: Hong Kong.

302 Müllenbach, R., Lagoda, P.J., Welter, C., 1989. An efficient salt-chloroform extraction of DNA from
303 blood and tissues. Trends Genet. 5, 391.

304 Pereira, A.M., Brito, C., Sanches, J., Sousa-Santos, C., Robalo, J.I., 2014. Absence of consistent genetic
305 differentiation among several morphs of *Actinia* (Actiniaria: Actiniidae) occurring in the Portuguese
306 coast. Zootaxa 3893, 595-600.

307 Pereira, A.M., Cadeireiro, E., Robalo, J.I., 2017. Asexual origin of brooding in the sea anemones
308 *Actinia equina* and *A. schmidtii*: molecular evidence from the Portuguese shore. N. Z. J. Mar. Freshw.
309 Res. 51, 316-320.

310 Perrin, M.C., Thorpe, J.P., Solé-Cava, A.M., 1999. Population structuring, gene dispersal and
311 reproduction in the *Actinia equina* species group. Oceanography and Marine Biology 37, 129-152.

312 Quicke, D.L.J., Brace, R.C., 1984. Evidence for the existence of a third, ecologically distinct morph of
313 the anemone, *Actinia equina*. J. Mar. Biol. Assoc. U.K. 64, 531-534.

314 Quicke, D.L.J., Donoghue, A.M., Brace, R.C., 1983. Biochemical-genetic and ecological evidence that
315 red/brown individuals of the anemone *Actinia equina* comprise two morphs in Britain. Mar. Biol. 77,
316 29-37.

317 Quicke, D.L.J., Donoghue, A.M., Keeling, T.F., Brace, R.C., 1985. Littoral distributions and evidence for
318 differential post-settlement selection of the morphs of *Actinia equina*. J. Mar. Biol. Assoc. U.K. 65, 1-
319 20.

320 Ratnasingham, S., Hebert, P.D.N., 2007. BOLD: The Barcode of Life Data System
321 (<http://www.barcodinglife.org>). Mol. Ecol. Notes 7, 355-364.

322 Rozas, J., Ferrer-Mata, A., Sánchez-DelBarrio, J.C., Guirao-Rico, S., Librado, P., Ramos-Onsins, S.E.,
323 Sánchez-Gracia, A., 2017. DnaSP 6: DNA sequence polymorphism analysis of large data sets. Mol.
324 Biol. Evol. 34, 3299-3302.

325 Schama, R., Solé-Cava, A.M., Thorpe, J.P., 2005. Genetic divergence between east and west Atlantic
326 populations of *Actinia* spp. sea anemones (Cnidaria: Actiniidae). Marine Biology 146, 435-443.

327 Schmidt, H., 1971. Taxonomie, verbreitung und variabilität von *Actinia equina* Linnt 1766 (Actiniaria;
328 Anthozoa). Zeitschrift für Zoologische Systematik und Evolutionsforschung 9, 161-169.

329 Shearer, T.L., van Oppen, M.J.H., Romano, S.L., Wörheide, G., 2002. Slow mitochondrial DNA
330 sequence evolution in the Anthozoa (Cnidaria). Mol. Ecol. 11, 2475-2487.

331 Sole-Cava, A.M., Thorpe, J.P., 1987. Further genetic evidence for the reproductive isolation of green
332 sea anemone *Actinia prasina* Gosse from common intertidal beadlet anemone *Actinia equina* (L.).
333 Mar. Ecol. Prog. Ser. 38, 225-229.

334 Song, J.-I., 1984. A systematic study on the Korean Anthozoa. 8. Actiniaria (Hexacorallia). J. Korean
335 Res. Inst. Better Living 34, 69-88.

336 Stephenson, T.A., 1935. The British sea anemones. The Ray Society, London.

337 Stothard, P., Wishart, D.S., 2005. Circular genome visualization and exploration using CGView.
338 Bioinformatics 21, 537-539.

339 Untergasser, A., Cutcutache, I., Koressaar, T., Ye, J., Faircloth, B.C., Remm, M., Rozen, S.G., 2012.
340 Primer3 - new capabilities and interfaces. Nucleic Acids Res. 40, e115.

341 Watts, P.C., Thorpe, J.P., 1998. Phenotypic identification of three genetically differentiated morphs
342 of the intertidal beadlet anemone *Actinia equina* (Anthozoa: Cnidaria). J. Mar. Biol. Assoc. U.K. 78,
343 1365-1368.

344 Westram, A.M., Rafajlović, M., Chaube, P., Faria, R., Larsson, T., Panova, M., Ravinet, M., Blomberg,
345 A., Mehlig, B., Johannesson, K., Butlin, R., 2018. Clines on the seashore: the genomic architecture
346 underlying rapid divergence in the face of gene flow. *Evol. Letters* 2, 297-309.

347 Yanagi, K., Segawa, S., Tsuchiya, K., 1999. Early development of young brooded in the enteron of the
348 beadlet sea anemone *Actinia equina* (Anthozoa: Actiniaria) from Japan. *Invertebrate Reproduction &
349 Development* 35, 1-8.

350 Zhang, L., Zhu, Q., 2017. Complete mitochondrial genome of the sea anemone, *Anthopleura midori*
351 (Actiniaria: Actiniidae). *Mitochondrial DNA Part A* 28, 335-336.

352

353 **Figure Legends:**

354 Figure 1:

355 Gene order in *Actinia equina* mitochondrial DNA (20,690bp). Figure produced in MTVIZ
356 (<http://pacosy.informatik.uni-leipzig.de/mtviz>). %AT is shown within the gene order diagram. Grey
357 shaded areas indicate intergenic regions.

358 Figure 2:

359 Collection sites for *Actinia equina* samples. For sample sizes refer to Table 1. The relative frequency
360 of the two haplotypes (Haplotype A: black; Haplotype B: light grey) is depicted in each pie chart. R =
361 red/orange pedal discs, G = green pedal discs, P = *A. prasina*.

362 Figure 3:

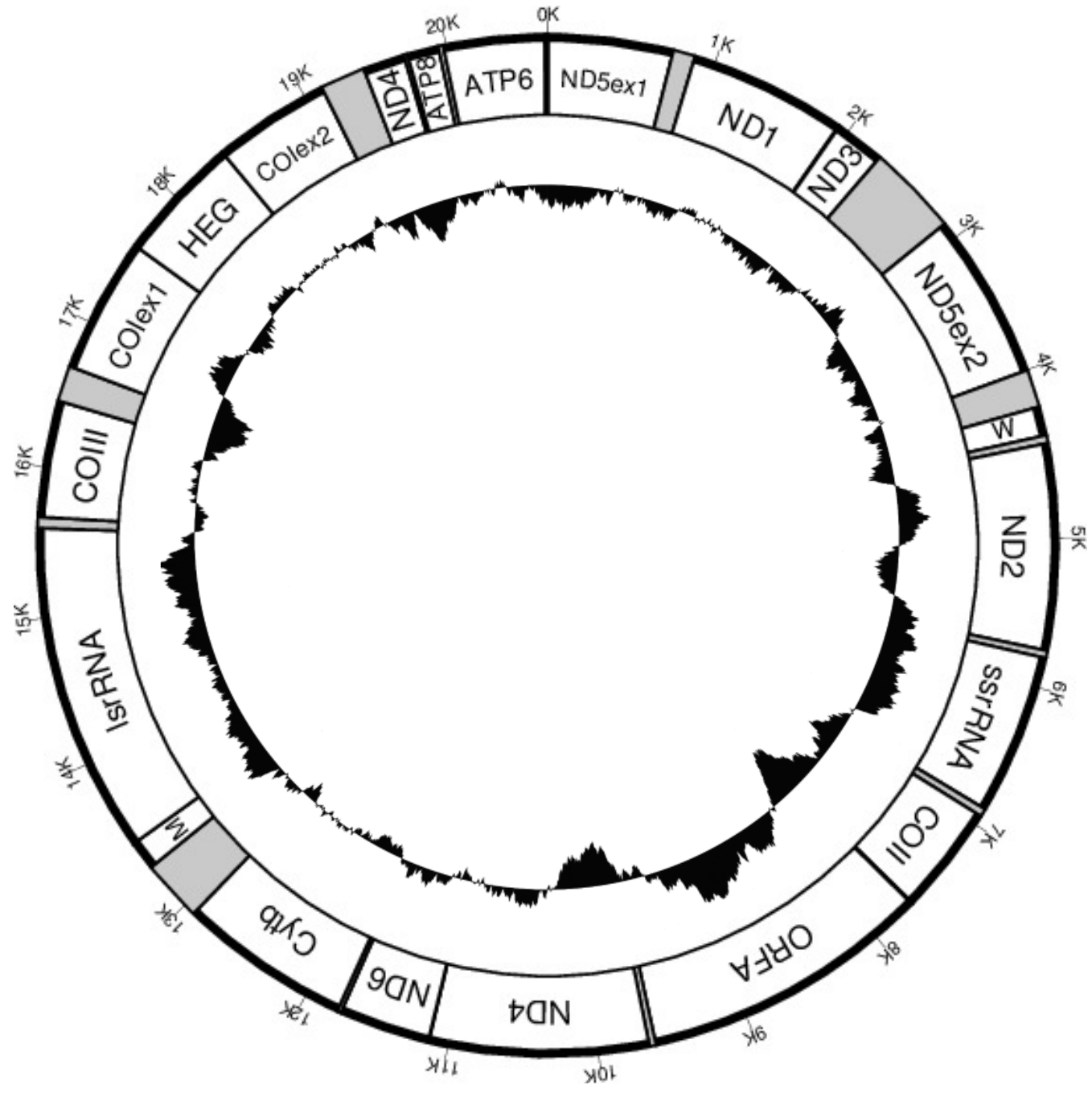
363 Sliding window analysis of the alignment of *Actinia equina* and *Anemonia viridis* mitochondrial
364 genomes. The line shows the value of nucleotide diversity (π) in a sliding window analysis of window
365 size 500 bp with step size 25 bp with the value plotted at its mid-point. Genes are displayed as grey

366 boxes below the x-axis. Genes with introns are labelled with *. Positions of amplified PCR products:
367 a) *COIII-COI* b) Folmer and c) *COI-ND4*. Figure drawn in OGDRAW (Lohse et al., 2013).

368 **Table 1: Haplotype distribution in geographic samples of *A. equina* and *A. prasina* from England,**
 369 **Wales, Scotland and the Isle of Man. Only two haplotypes are found, Haplotype A (accession**
 370 **MH636618) and Haplotype B (MH636619), differing by 1bp.**

| | | Haplotype A | Haplotype B |
|-------------------------------------|-------------------|-------------|-------------|
| Millport, Isle of Cumbrae, Scotland | Green | 0 | 2 |
| | Orange | 3 | 0 |
| | Red | 1 | 1 |
| Peel, Isle of Man | Green | 0 | 1 |
| | Red | 1 | 0 |
| | <i>A. prasina</i> | 0 | 1 |
| Niarbyl, Isle of Man | Red | 0 | 1 |
| New Brighton, Wirral, England | Green | 0 | 2 |
| | Red | 0 | 4 |
| | <i>A. prasina</i> | 0 | 2 |
| Llandudno, North Wales | Green | 0 | 2 |
| | Red | 2 | 0 |
| Holyhead, Anglesey, North Wales | Green | 0 | 3 |
| | Red | 2 | 0 |
| Rhosneigr, Anglesey, North Wales | Green | 0 | 2 |
| | Red | 2 | 0 |
| St Brides Bay, South Wales | Green | 0 | 4 |
| | Red | 2 | 2 |
| Marloes, South Wales | Green | 0 | 3 |
| | Red | 3 | 0 |

371



R G P



Millport



Peel



Niarbyl



New Brighton



Llandudno



Holyhead



Rhosneigr



St Bride's Bay



Marloes



